E13-2002-14

A. Yu. Petrus

MULTIWIRE PROPORTIONAL CHAMBER WITH A DIELECTRIC FILM. NUMERICAL STUDY

1 Introduction

New experiments being conducted and planned on accelerators impose heavy demands on the used track detectors. In particular, proportional chambers are required to have stable and long period of operation at high counting rates as well as to have a small dead time, contain a small amount of substance on the way of registered particles and at the same time providing a high detection efficiency, covering considerable areas ($\gtrsim 1000cm^2$). As is shown in [1], reduction of the wire step to improve the coordinate resolution of the chamber leads to limitations imposed on the allowable wire length, which are connected with the instability of the wire as to its attraction to the cathode. On the other hand, the dimensions of the sensitive area of one of the proportional chambers in the forward detector of the ANKE spectrometer [2] are $58cm \times 49cm$. From [1] it follows that with the required step $1mm$, the wires in such a chamber will be unstable at the standard geometry. That is why there have been developed and produced chambers with wires lying on a dielectric film, as is shown in Fig.1 [3]. The film surface opposite to the wire side is covered with a conductive silver paint. from now on it will be referred to as strip surface. To avoid accumulation of the positive charge on the film, which would distort the electric field and lead to an amplification drop, the film was made of a material with a small conductivity $\gamma \sim 10^{-9}\Omega^{-1}cm^{-1}$. This allowed a sufficiently quick evacuation of the positive ions from the film surface, thus retaining the chamber operation at high counting rates. The technology of preparing a film and constructing such chambers, their working characteristics as well as results of their performance in experiments will be dwelled on in other publications. This particular work is devoted to a numerical investigation of electrostatics of such chambers as well as to the impact of various factors on their working characteristics.

2 Field equations

In the case of an ideal dielectric, the potential of the electrostatic field ϕ obeys the equation

$$\nabla(\epsilon\nabla\phi) = -\rho, \tag{1}$$

where ϵ is the dielectric constant of the medium, ρ is the space density of a free charge. In the absence of space charges and in a uniform medium, (1) reduces to the Laplace equation

$$\Delta\phi = 0, \tag{2}$$

and the electric field strength is defined by the potential gradient

$$\vec{E} = -\nabla\phi. \tag{3}$$

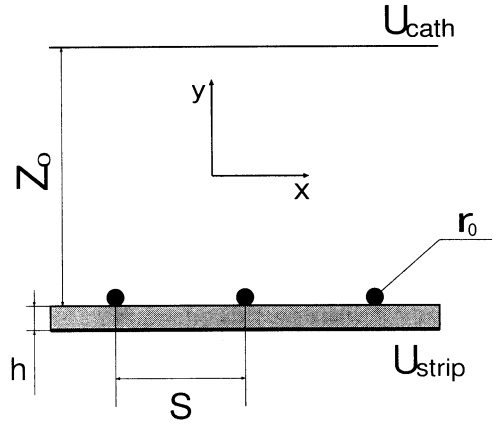

Figure 1: A proportional chamber with a dielectric film.

In the presence of a boundary between two media with the dielectric constants ϵ_1 and ϵ_2 correspondingly, there must be conditions of conjugation imposed on it:

$$(\epsilon_2 \vec{E}^{(2)} - \epsilon_1 \vec{E}^{(1)}) \cdot \vec{n} = \sigma, \tag{4}$$

$$(\vec{E}^{(2)} - \vec{E}^{(1)}) \times \vec{n} = 0, \tag{5}$$

where σ is the surface charge and $\vec{n}$ is the unit vector perpendicular to the boundary and pointing from region 1 to region 2. In the absence of the surface charge condition (4) reduces to

$$(\epsilon_2 E_\perp^{(2)} - \epsilon_1 E_\perp^{(1)}) = 0, \tag{6}$$

where $E_\perp$ is the field component perpendicular to the boundary of two dielectrics.

In the case of an isotropic linear conducting medium, the field strength is connected with the current density by the Ohm law:

$$\vec{j} = \gamma \vec{E}, \tag{7}$$

where γ is the conductivity of the medium. Taking into account (3) and applying the divergence operator to both parts of the previous equation, we obtain:

$$-\nabla \cdot (\gamma \nabla \phi) = \mathrm{div}\vec{j}. \tag{8}$$

The terms on the right side of the equation refer to the density of current sources in the medium and in their absence this equation reduces once again to the Laplace equation (2). In the general case of a boundary between two conductive

media with the conductivity γ_1 and γ_2 correspondingly, as well as in the absence of current sources, two conditions are fulfilled:

$$E_{||}^{(1)} = E_{||}^{(2)}, \tag{9}$$

$$\gamma_1 E_{\perp}^{(1)} = \gamma_2 E_{\perp}^{(2)}. \tag{10}$$

The first condition expresses continuity of the tangent component of the field strength, whereas the second one refers to the continuity of the normal component of the current density on the boundary of the media. In the case when one of the media is non-conductive ($\gamma_2 = 0$), the second condition reduces to $E_{\perp}^{(1)} = 0$. This is easy to understand bearing in mind that in a stationary situation the current does not flow through the boundary between a conductor and a dielectric. Thus, boundary conditions for a conducting film have been completely specified and the Laplace equation in it can be solved independently. After the potential inside the conductive film has been found, one may pass on to solving the Laplace equation in the other part of the chamber. Conditions for the boundary between the film and gas follow from the continuity of the potential: $\phi^{(1)} = \phi^{(2)}$.

It is necessary to note, that from these equations it follows that the field in the chamber in the stationary case is dependent neither on the dielectric constant of the film material, nor on its conductivity. These properties of the film affect only dynamic characteristics. The above-mentioned problem will be discussed later on.

Solution of these boundary-value problems was carried out using the finite-difference method on the grid sequence with a decreasing step. At first the solution was obtained on a rough grid, then it was transferred onto a smaller grid by means of interpolation and used as an initial approximation for the iterative method. Near the points of the curved boundary a non-uniform grid was used [4]. This leads to a second order approximation at the inner points of the grid and keeps both symmetry and positive definiteness of the difference problem matrix. These properties of the matrix allow the use of the successive over-relaxation iteration method:

$$\mathbf{\Phi}^{n+1} = (1-\omega)\mathbf{\Phi}^n + \omega(\boldsymbol{T}\mathbf{\Phi}^n + \boldsymbol{F}), \tag{11}$$

where $\mathbf{\Phi}^n$ is the approximation to the problem's solution at a n-iteration, $\boldsymbol{F}$ is the vector of the right-hand sides, $\boldsymbol{T}$ is the transition matrix and ω is the iterative parameter. To achieve a faster convergence, an iterative parameter ω close to the optimal one was selected in the course of counting [5].

3 Results of calculations

Fig.2 shows the distribution of the field strength in the chamber, the field lines are given in Fig.3. In this figure, the density of the field lines is proportional to the

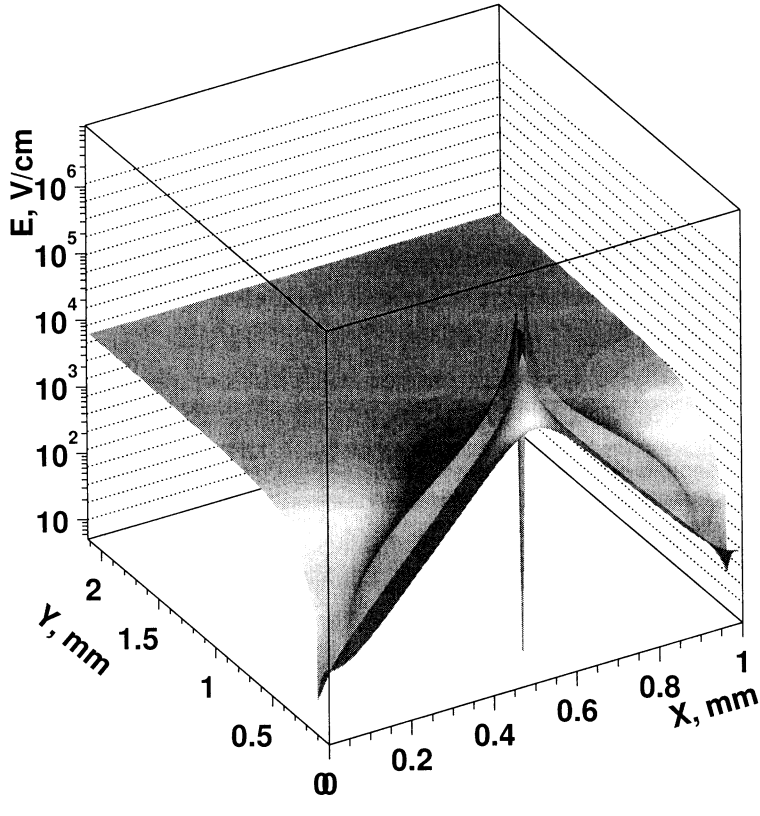

Figure 2: Electric field in the chamber with parameters $z_0 = 2.0mm$, $s = 1.0mm$, $h = 0.1mm$, $U_{cath} = -2700V$, $U_{strip} = -1700V$.

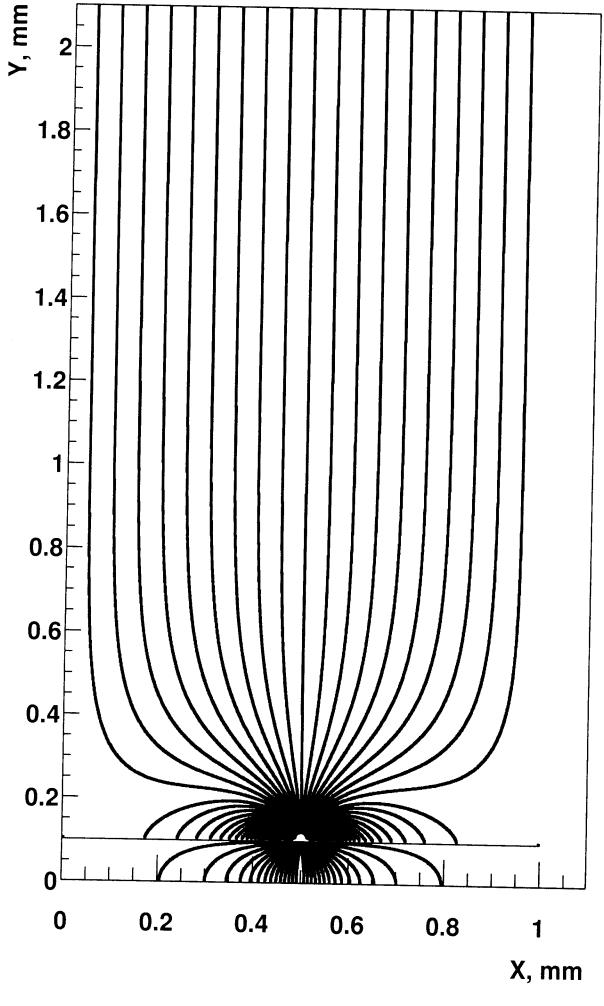

Figure 3: Field lines in the chamber. Chamber parameters are the same as for Fig.2. The density of the field lines is proportional to the field strength.

field strength. It is necessary to note, that there is an area near the boundary of the chamber cell with the field lines going not to the wire, but to the film surface. Thus, electrons produced in this area as a result of ionization by a passing particle, will not reach the anode wire and will not induce avalanche formation. Let us assume that tracks cross the chamber perpendicularly to the wire plane. Tracks crossing the area from which electrons drift towards the anode wire will be considered as geometrically efficient. The relative number of such tracks will be called geometrical efficiency. For example, in a case referring to Fig.2, geometrical efficiency amounted to $\sim 99.2\%$. From an analysis of initial equations it is easy to see that the configuration of field lines and therefore the geometrical efficiency depend only on the ratio of the potentials at the cathode and strips, but is not dependent on the absolute values of the potentials. Fig.4 shows the chamber geometrical efficiency as a function of the ratio of the potentials at the electrodes. With the ratio $U_{strip}/U_{cath} \simeq 0.65$, the geometrical efficiency reaches a value exceeding 99.7%. It is also easy to see, that with an increased gap between the cathode and the wires and with an invariable step of wires, the geometrical efficiency also increases.

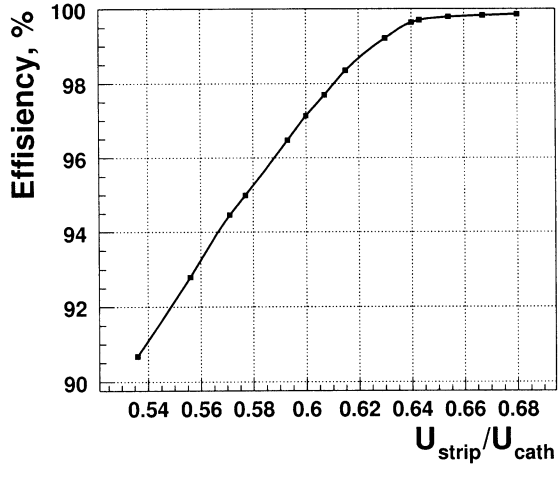

Figure 4: Geometrical efficiency of the chamber with $z_0 = 2.0mm$, $s = 1.0mm$, $h = 0.1mm$ as a function of U_{strip}/U_{cath}.

From the configuration of the field lines in the chamber, it becomes clear that part of the positive ions, left after the avalanche electrons moved onto the wire, will drift not towards the cathode, but towards the dielectric film. Thus, part of the ions, instead of drifting the whole way towards the cathode (about

$2mm$), move to the film and their paths do not exceed $250\mu m$. This leads to a reduced relaxation time of the residual space charge around the wire, and thus to increasing chamber counting rates. The area from which the ions drift towards the film is shown in Fig.5. In the same figure the avalanche formation area is given for comparison. As is seen, the overlap of these areas covers about half the avalanche formation area. Due to the electron diffusion over the avalanche formation area, about half the produced ions will drift towards the film.

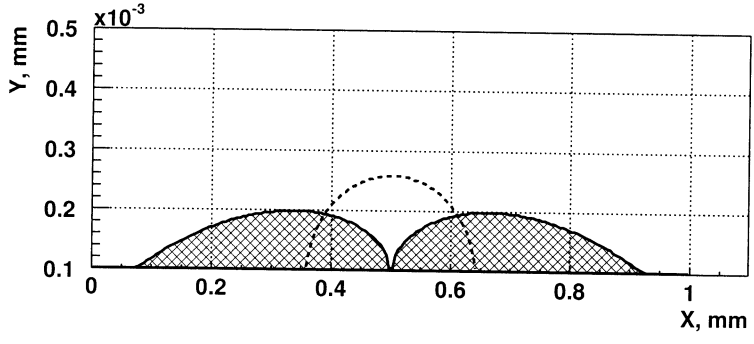

Figure 5: Line separating two areas from which ions drift to the film and to the cathode correspondingly (solid line). The dashed line shows the avalanche formation region ($E > 20kV/cm$).

4 Amplitude characteristics of the chamber

In this part the impact of various chamber parameters on the gas amplification will be considered. The above mentioned methodic allows calculating the field at any point of the chamber. Bearing in mind the dependence of the Townsend first coefficient α on the field strength, gas amplification is possible to calculate according to the formula

$$G = \exp(\int \alpha(E)dl), \tag{12}$$

where integration is carried out along the electron drift path (that is along the field line). It is clear that this formula does not take into account the influence of the avalanche space charge, which becomes noticeable at a higher amplification ($\gtrsim 5 \cdot 10^5$), the influence of electron diffusion, as well as the statistical character of cluster formation along the particle trajectory. Nevertheless, this formula is suitable for calculations if it is considered as an approximation which allows evaluating the impact of various factors on the amplification in the chamber.

Evaluation of the gas amplification was based on the data for α from [6]. Fig.6 shows the gas amplification as a function of the point of creation of a primary electron. As is seen, the amplification coefficient can differ by almost a factor of two, which, in its turn, will lead to a broader amplitude distribution in the chamber. For comparison the same dependence is given for a chamber without a dielectric film. This dependence is of the opposite character, but the amplification coefficient differs by a factor of two as well. Thus, the amplitude distribution in a chamber with a dielectric film is not expected to differ greatly from the amplitude range of a usual chamber.

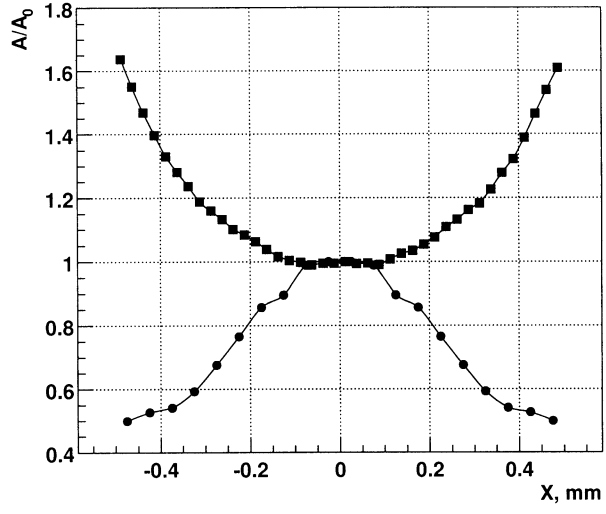

Figure 6: Amplification in the chamber with $z_0 = 2.0mm$, $s = 1.0mm$, $h = 0.1mm$ as a function of the point of creation of the primary electron (■). For comparison the same dependence is given for a usual proportional chamber without a dielectric film with the same gap and step [1].

A more realistic description of the amplification can be achieved by taking into account the statistical character of cluster formation along a particle trajectory (see Fig.7). Let us assume that a particle crosses the chamber at an angle of θ. Then the total length of the track inside the gas gap in the chamber is equal to $d = z_0 \cos(\theta)$. The track may cross several neighboring chamber cells. In this case, electrons produced as a result of ionization will drift towards different wires. Let us consider the amplitude characteristics of a single cell. Let us assume that the counting rate is uniform over the chamber and the tracks cross the chamber

at angles in the interval $-10^0 \leq \theta \leq 10^o$, with a track making a contribution into the amplitude distribution only if half the track belongs to the given cell. Thus, we exclude the cases when a track only touches the cell, with its major part lying in the neighboring cell. As is known, clusters are distributed along the track according to Poisson's law

$$P(n) = \frac{(\mu d)^n \exp(-\mu d)}{n!}, \tag{13}$$

where $P(n)$ is the probability of production of n electrons on a track with a length d, μ is the number of electrons per track length unit created by a passing particle. As is known, for the gas CF_4 $\mu = 51\text{cm}^{-1}$ [7]. In Fig.8 an example of amplitude distributions, obtained by the above-mentioned method, is given for chambers with a dielectric film and without it. As could be expected from Fig.6, the widths of the distributions are approximately equal.

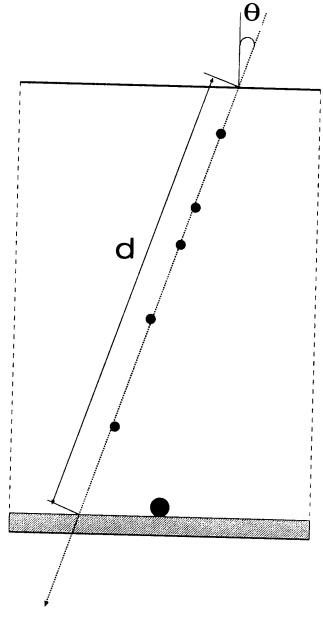

Figure 7: Cluster formation along the particle track.

Fig.9 shows the most probable amplitude as a function of the voltage at the strips and cathode. As is clearly seen from the figures, with an increase of the voltage by 300V at the strips, the amplitude increases by a factor of more than 10, whereas the amplitude increase amounts to 30% with the same increase of the voltage at the cathode. Apart from that, the growth of amplitude along with

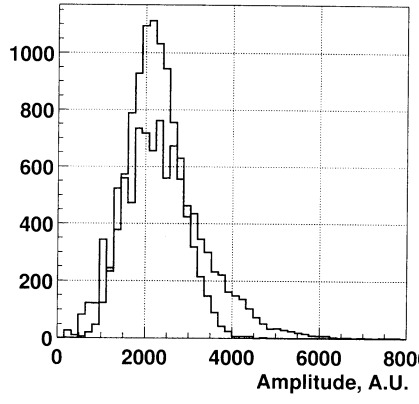

Figure 8: An example of amplitude distributions for MWPC with a dielectric film (empty histogram) and for a chamber without it (shaded histogram).

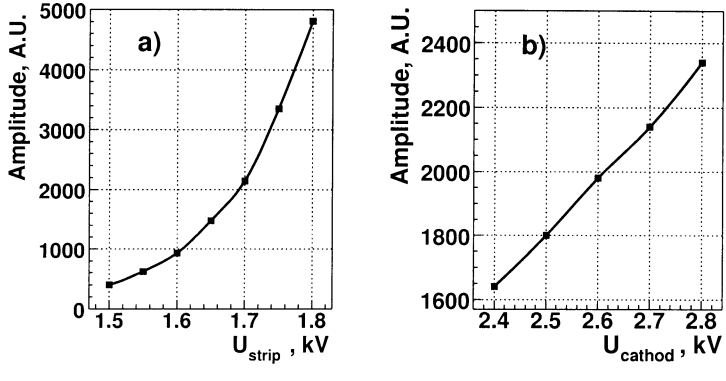

Figure 9: Most probable amplitude for MWPC with a film as a function of strips voltage (a) and cathode voltage (b).

the growth of voltage is exponential for the strips, whereas this growth for the cathode is only linear. This indicates that the decisive factor for the amplification is the voltage at the strips, with the voltage at the cathode conditioning only the drift of the primary electron.

As the wire lies on a dielectric film and it is influenced by the electrostatic forces from the strips, the wire is expected to be to one extent or another pressed in the film. Let us evaluate the forces acting on the wire. The linear density of the charge on the wire can be calculated by integrating the field strength along the closed curve enveloping the wire at a small distance from it:

$$\eta = 2\pi\epsilon_0 \int \vec{E} \cdot \mathrm{d}\vec{l}. \tag{14}$$

With $U_{cath} = -2700V$ and $U_{strip} = -1700V$ the calculation of the integral leads to the value $\eta = 4.6 \times 10^{-7} Q/m$. On the other hand, the density of the charge on the film is calculated analogously:

$$\sigma(x) = \epsilon_0 \vec{E}(x, y = h + 0) \cdot \mathrm{d}\vec{n_s} = E_y(x, y = h + 0), \tag{15}$$

where $\vec{n_s}$ is the unit vector normal to the surface, with the expression $E(x, y = h + 0)$ to be understood as the value of the field directly above the film. Fig.10 shows the distribution of the surface density of the charge near the wire. Thus, the force acting on the wire is possible to evaluate according to the formula:

$$F = \frac{\eta}{2\pi\epsilon_0} \int \frac{\sigma(x)}{r(x)} \mathrm{d}x, \tag{16}$$

where $r(x)$ is the distance between the point with the coordinate x on the film surface and the center of the wire. Upon substituting the known values for η and $\sigma(x)$, the calculations give $F \simeq 6N/m$.

Bearing in mind the force with which the wire acts on the film, it is possible to evaluate the value of the wire pressing into the film according to formula [8]

$$\Delta h = \frac{4F}{\pi^2 K} \ln(r_0/h), \tag{17}$$

where K is the Young modulus of the film material, r_0 is the wire radius, h is the film thickness. If the Young modulus of the film equals $2 \cdot 10^8 Pa$ (polyethylene), then $\Delta h \simeq 0.1 \mu m$. When such a chamber is operated, a mixture containing isopropylene alcohol vapor is blown through the chamber to provide the necessary film conductivity. As the film is saturated with the alcohol and becomes friabler, its Young modulus may become lower than that of the dry one. That is why the pressing-in value can be significantly greater. Fig.11 shows the most probable amplitude and amplitude resolution as a function of the value of the wire pressing into the dielectric film. As is seen, at first the amplitude decreases until $\sim 75\%$,

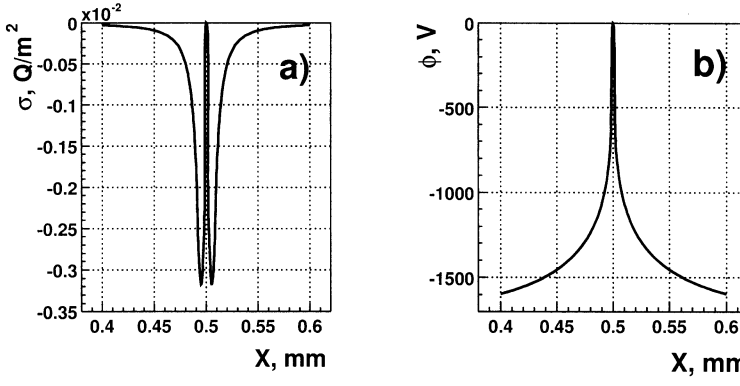

Figure 10: a) Surface density of the charge of the film near the wire; b) value of the potential of the electric field near the film. $U_{cath} = -2700V$ $U_{strip} = -1700V$.

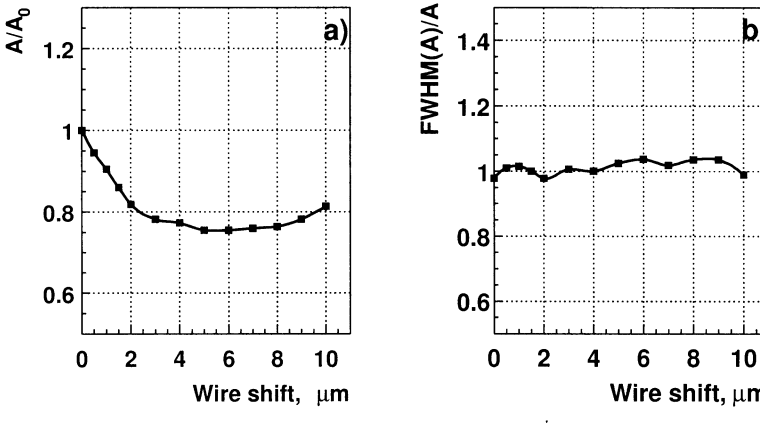

Figure 11: Most probable amplitude (a) and amplitude resolution (b) as a function of the wire pressing into the film.

but then it remains approximately at the same level. As far as the amplitude resolution is concerned, it is practically not dependent upon the degree of the wire pressing into the film. It is important to note that in the calculations the counting rates were implicitly supposed to be low, that is charge accumulates neither around the wire, nor on the film. At high counting rates the charge accumulated on the film, without enough time for evacuation due to the low conductivity of the film, will influence the electric field configuration, and thus, the amplification. The charge relaxation time can be evaluated in the following way. From equations (1) and (8) it follows that

$$\mathrm{div}\vec{j} = \frac{\gamma}{\epsilon}\rho. \tag{18}$$

Bearing in mind that $\mathrm{div}\vec{j} = -\partial\rho/\partial t$, we get

$$\rho = -\frac{\gamma}{\epsilon}\partial\rho/\partial t, \tag{19}$$

therefore, the charge evolution in the film obeys the following law:

$$\rho(t) = \rho_0 \exp\left(-\frac{\gamma}{\epsilon}t\right), \tag{20}$$

where ρ_0 is an initial charge distribution. The typical value of the dielectric constant for the film material is $3 \div 5\epsilon_0$ and the conductivity is $10^{-7}\Omega^{-1}m^{-1}$. Thus, the characteristic time of charge relaxation is $\tau \sim 3 \cdot 10^{-4}s$. Taking into account that the transverse avalanche size is about $100\mu m$ owing to diffusion and that the counting rate is stable, we get that the counting rate for $1cm$ of wire, giving rise to a significant influence of the charge accumulated on the film, is equal to $\sim 3 \cdot 10^5 s^{-1}$. Or, for a chamber with the step $1mm$ the critical counting rate $\sim 3 \cdot 10^6 s^{-1}cm^{-2}$. It is necessary to note that such a consideration does not take into account the field distortion, which is due to the charge accumulated on the film.

The influence of the charge accumulated on the film can be evaluated in the following way. Let the average amplification in the chamber be equal to A. Then the total charge accumulated in a time unit on a wire length unit equals

$$C_1 = AeN, \tag{21}$$

where e is the electron charge, N is the counting rate per a wire length unit. The rate of ion evacuation due to the film conductivity equals

$$C_2 = \rho/\tau_0, \tag{22}$$

where ρ is the charge accumulated on the film per a wire length unit. Stationary conditions can be written in the form of equality $C_1 = C_2$. For evaluation one may assume that the charge is distributed around the wire according the Gaussian law.

Taking into account (21) and (22), the following can be written for the surface density of the charge accumulated around the wire:

$$\sigma(x) = \frac{AeN\tau_0}{\Delta x\sqrt{2\pi}} \exp(-\frac{(x - x_w)^2}{2(\Delta x)^2}), \tag{23}$$

where Δx characterizes the width of charge distribution around the wire. It is seen from Fig.5 that for a chamber with one millimeter step one can assume $\Delta x \simeq 100\mu m$. It is necessary to note that with account of additional charge on the film the field in the chamber cannot be calculated in the form of superposition of the field in the absence of accumulated charge on the film and the field produced by this charge. This is conditioned by the fact that additional charge on the film would influence the value of charge induced on the wire and thus change the chamber "unperturbed" field. To calculate the field in this case, it is necessary to solve the Laplace equation once again, but this time with boundary conditions taking into account the current from the film surface. Charge leaving a surface unit in a time unit is equal to $\sigma(x)/\tau_0$. Then, taking into consideration the Ohm law, for the Laplace equation in the film the boundary condition on the boundary between the film and gas can be presented in the form

$$\vec{E}_\perp(x, y = h - 0) = \frac{\gamma}{\tau_0}\sigma(x). \tag{24}$$

As this boundary condition influences only the vector of the right side of (11) and the transition matrix remains unchanged, the method of successive over-relaxation can be applied once again to solve the difference problem.

Fig.12(a) shows the linear density of the charge induced on the wire as a function of the chamber counting rate. The values of voltage at the cathode and strips are selected in such a way that amplification amounts to $5 \cdot 10^5$ at low counting rate when the influence of accumulated charge can be neglected. Such amplification allows one to neglect the influence of the avalanche field on the avalanche development. As is seen from the figure, increased counting rate leads to an increase of the accumulated charge on the film, which in its turn decreases charge induced on the wire. This leads to a drop in amplification. Fig.12(b) shows the most probable amplitude as a function of the chamber counting rate. It is clear that the amplification drop value also depends on the absolute value of amplification. With higher amplification the influence of counting rate on the chamber amplitude characteristics takes place earlier.

5 Conclusion

In this paper electrostatic properties of multiwire proportional chambers with a dielectric film of a low conductivity $\gamma \sim 10^{-7}\Omega cm$ have been considered. Distribution of the field strength in the chamber and configuration of the field lines have

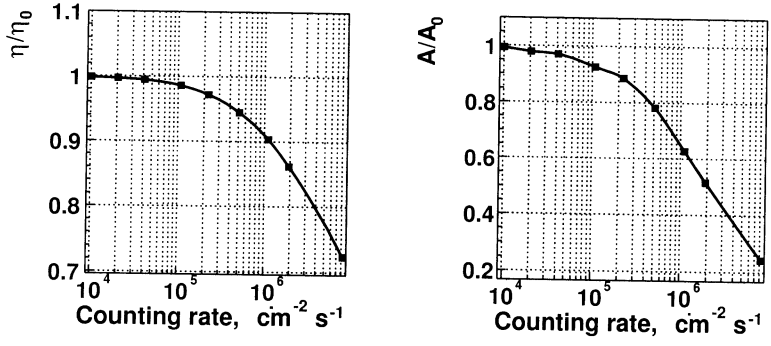

Figure 12: Linear density of the charge induced on the wire (a) and the most probable amplitude (b) as a function of chamber counting rate. η_0 and A_0 are the linear density of the charge and amplitude at low counting rate when the influence of the charge accumulated on the film can be neglected.

been obtained. The amplitude characteristics of such chambers have also been investigated. It is necessary to note that in so doing, the influence of the avalanche space charge was not taken into account (which is valid up to the amplification $\sim 5 \cdot 10^5$) as well as the influence of the avalanche diffusion. In the framework of this model it was shown that the amplitude distribution for a chamber with a film did not differ much from the distribution in a usual chamber. The major influence on the value of amplification is exerted by the value of voltage applied to the strips. The influence of the cathode voltage value is considerably weaker. Generally its role is to provide the necessary velocity of the drift of primary electrons. As far as the counting rate characteristics are concerned, the calculations showed that at an amplification up to $\sim 5 \cdot 10^5$ the chamber continued working up to the counting rate $\sim 5 \cdot 10^5 cm^{-2} s^{-1}$, if a 20% drop in the amplitude was regarded as allowable in comparison with the signal amplitude at low counting rate.

I would like to thank Dr. B.Zh.Zalikhanov for intensive discussions on the subject of this paper. Also I am grateful to Prof. V.I.Komarov for a careful reading of the manuscript and valuable comments.

References

[1] A.Yu.Petrus, B.Zh.Zalikhanov, "Electro-mechanical properties of narrow-gap multiwire proportional chambers", **E13-2001-113, (2001), JINR**, accepted for NIM A.

[2] S.Barsov et al., **NIM A462 (2001) 364.**

[3] V.Komarov et al., "First Module of the Forward Detector Proportional Chambers of the ANKE Spectrometer", 1995 IKP Annual Report, KFA Jülich (1996) p.67.

[4] A.A.Samarskiy, "Theory of Difference Schemes". (in Russian) "Nauka", Moscow, 1985.

[5] Il'in, "Numerical Methods of Electrophysical Problems Solving" (in Russian) "Nauka", Moscow, 1985.

[6] L.G.Christophorou and J.K.Olthoff, "Electron interaction with plasma processing gasses: An update for CF_4, CHF_3, C_2F_6 and C_3F_8", **J.Phys.Chem.Ref.Data, 28 (1999) 967.**

[7] J.Va'vra, "Wire chamber gases", **NIM A323 (1992) 34.**

[8] S.P.Timoshenko, D.Gudier, "Theory of Elasticity","Mir", Moscow, 1975.

Received on February 1, 2002.

Петрус А. Ю.
E13-2002-14

Многопроволочные пропорциональные камеры
с диэлектрической подложкой.
Численное моделирование

Рассмотрена электростатика многопроволочной пропорциональной камеры с диэлектрической подложкой, обладающей слабой проводимостью. Численными методами получено распределение электрического поля в камере. Это позволило исследовать влияние различных параметров (геометрия камеры, напряжение на электродах) на рабочие характеристики камеры. Также получена зависимость амплитудных характеристик камеры от ее загрузки.

Работа выполнена в Лаборатории ядерных проблем им. В. П. Джелепова ОИЯИ.

Сообщение Объединенного института ядерных исследований. Дубна, 2002

Petrus A. Yu.
E13-2002-14

Multiwire Proportional Chamber with a Dielectric Film.
Numerical Study

Electrostatical properties of multiwire proportional chambers with a dielectric film of a low conductivity are considered. Distribution of the electric field in the chamber was obtained using numerical methods. This allowed investigating the influence of various parameters (chamber geometry, voltage at the electrodes) on the chamber working characteristics. Dependence of the chamber amplitude characteristics on the counting rate was also obtained.

The investigation has been performed at the Dzhelepov Laboratory of Nuclear Problems, JINR.

Communication of the Joint Institute for Nuclear Research. Dubna, 2002

Макет *Т. Е. Попеко*

ЛР № 020579 от 24.06.97.
Подписано в печать 07.02.2002.
Формат 60 × 90/16. Бумага офсетная. Печать офсетная.
Усл. печ. л. 1,18. Уч.-изд. л. 1,32. Тираж 315 экз. Заказ № 53101.

Издательский отдел Объединенного института ядерных исследований
141980, г. Дубна, Московская обл., ул. Жолио-Кюри, 6.